Available online at www.sciencedirect.com

SCIENCE DIRECT®

International Journal of Multiphase Flow

PERGAMON

International Journal of Multiphase Flow 29 (2003) 1221–1236

www.elsevier.com/locate/ijmulflow

The control of micro-air-bubble generation by a rotational porous plate

Shigeo Fujikawa [a], Rongsheng Zhang [b], Shinji Hayama [b], Guoyi Peng [b,*]

[a] *Division of Mechanical Science, Graduate School of Engineering, Hokkaido University, North 13, West 8, Kita-Ku, Sapporo 060-8628, Japan*

[b] *Department of Mechanical Systems Engineering, Faculty of Engineering, Toyama Prefectural University, Kurokawa 5180, Kosugi-machi, Imizu-gun, Toyama 939-0398, Japan*

Received 4 October 2002; received in revised form 14 May 2003

Abstract

This paper is concerned with methods of generation, control and measurement of micro-air-bubbles in water. A new device for the generation of micro-air-bubbles is developed on the basis of dissolution and separation processes of air in water. In the dissolution process, air is dissolved in water in such an efficient way that compressed air is ejected into water in the form of numerous small bubbles from a rotating circular porous plate and that the mixture of water and generated air bubbles is stirred in the following mixing box where air bubbles dissolve into the surrounding water. In the succeeding separation process, the air-dissolved water is discharged through a pressure reduction valve, after which the dissolved air becomes supersaturated and then the air is separated in the form of micro-air-bubbles. The diameter and the number density of separated micro-air-bubbles are controlled by adjusting both the rotational frequency of the porous plate and the flow rate of air ejected into water so as to change the amount of air dissolution in water. Experimental results show that the mean diameter of micro-air-bubbles is controlled between 10 and 20 μm, and the number density between 1.3×10^2 and 6.6×10^2 number/mm^3.

Keywords: Gas–liquid two-phase flow; Bubbly water; Micro-air-bubble generation; Rotating porous plate; Air dissolution; Bubble separation

* Corresponding author. Tel.: +81-766-56-7500x389; fax: +81-766-56-6131.
E-mail address: peng@pu-toyama.ac.jp (G. Peng).

0301-9322/03/$ - see front matter
doi:10.1016/S0301-9322(03)00106-X

1. Introduction

Mixtures of water and micro-bubbles have been used in many industrial fields for such purposes of purification of waste water, sterilization and decolorization of water, and food processing etc. (Iguchi and Chihara, 1997). Until the present, several methods for the generation of micro-bubbles in water have been developed, and they may be mainly classified into the following four kinds: (a) method using nozzles or porous materials (Miyahara et al., 1991), (b) method by stirring of water and bubbles (Onari, 1997; Cheremisinoff, 1985), (c) method by dissolution and separation of gas in water (Takahashi et al., 1979), (d) method by consecutive dissolution and separation of gas in water (Machitani et al., 1995).

In the methods of (a), (b) and (c), the mean diameter of generated micro-air-bubbles is larger than 50 μm and the number density is less than 10 number/mm^3. In the method of (d), however, the diameter and the number density are respectively 20 μm and 200 number/mm^3, the respective values are smaller and larger than those in the other three methods. For further extensive applications of industrial practices, it is now requested that the mean diameter is as smaller as possible and the number density is as higher as possible, and moreover, they are controllable according to purposes of application practices.

In the present paper, a new type of micro-air-bubble generator is proposed in order to meet the requirements mentioned above on the size and the number density. A Venturi nozzle used to suck air in the method (d) is replaced by a circular porous plate rotating at a changeable rotational frequency in a bubble dispersion box. Compressed air is ejected into the water in the form of numerous small air bubbles through small holes on the plate. The size of air bubbles can be changed by the rotational frequency of the plate. The bubble generation process in the dispersion box is analyzed theoretically, and the air dissolution process in the succeeding mixing box is discussed on the basis of experiments. Experimental results of micro-air-bubble generation in the following separation process show that the mean diameter of air-bubbles in water becomes much smaller and the number density does higher compared with those obtained by the other methods. The diameter and the number density are found to be controllable to a certain extent by changing the rotational frequency of the porous plate and the air flow rate through the plate.

2. Experimental apparatus and experimental methods

2.1. Micro-air-bubble generator

Fig. 1 shows the schematic diagram of the micro-air-bubble generator used in the present experiment. The generator consists of the following sections; air intake section (①–⑤), water supply section (⑥–⑧), bubble dispersion section (⑨), air dissolution section (⑩–⑫), exhaust section of insolvable air (⑬, ⑭), and micro-air-bubble separation section (⑯) after pressure reduction valve (⑮). The air intake and water supply sections are connected to the bubble dispersion box in which small air bubbles are generated on the surface of a rotating porous plate and the bubbles are fully dispersed in the water. Two kinds of porous plates are adopted: One with 126 holes of 0.14 mm in diameter and the other with 648 holes of 0.13 mm in diameter. These plates are 70 mm in diameter and 0.8 mm in thickness. The air dissolution section consists of the mixing

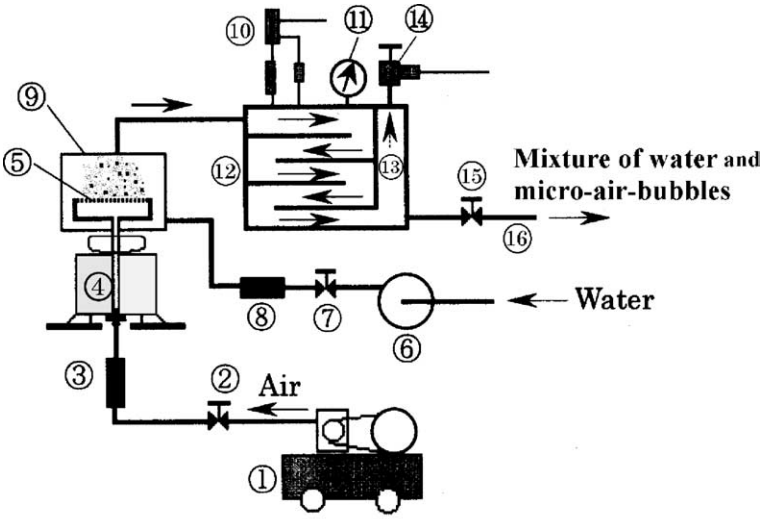

① Air compressor
② Regulator
③ Air flow gauge
④ Motor with shift gear
⑤ Porous Plate
⑥ Water pump
⑦ Regulator
⑧ Water flow gauge
⑨ Bubble dispersion box
⑩ Safety valve
⑪ Pressure gauge
⑫ Mixing box
⑬ Exhaust of insolvable air
⑭ Exit valve of insolvable air
⑮ Reduction valve
⑯ Separation tube

Fig. 1. Schematic diagram of experimental apparatus.

box (⑫), the safety valve (⑩) and the pressure gauge (⑪). The mixing box is a five-stages channel with the rectangular section of 20 mm in height and 25 mm in width. The total length of the channel is 1000 mm. The exhaust section consists of the vertical exhaust channel (⑬) and the exit valve (⑭). In the bubble separation section (⑯), the pressure reduction valve (⑮) is set to control the flow rate of bubbly water. The distance from the valve to the exit is 160 mm.

Micro-air-bubbles are generated through the following procedure by the generator mentioned above. Compressed air is ejected into water through small holes on the porous plate. In order to make bubbles generated from these small holes as smaller as possible, the plate is rotated to tear the bubbles in suitable sizes. The torn bubbles are fully dispersed into water in the dispersion box, and the mixture of water and bubbles is transported to the succeeding mixing box where the flow is in fully turbulent state and the bubbles dissolve into the water as they move downwards. Because the degree of air dissolution in the water has a great influence on the separation of micro-air-bubbles in the following separation process, it is important to be able to change the air dissolution degree in order to control the size of micro-air-bubbles and their number density. The dissolution degree can be controlled by changing the size of bubbles formed on the porous plate because the smaller are the bubbles, the more efficiently they dissolve. Undissolved air is discharged from the exhaust valve. The water with dissolved air is decompressed through the pressure reduction valve after which it becomes supersaturated with air and the dissolved air in the water separates in the form of micro-air-bubbles in the separation section.

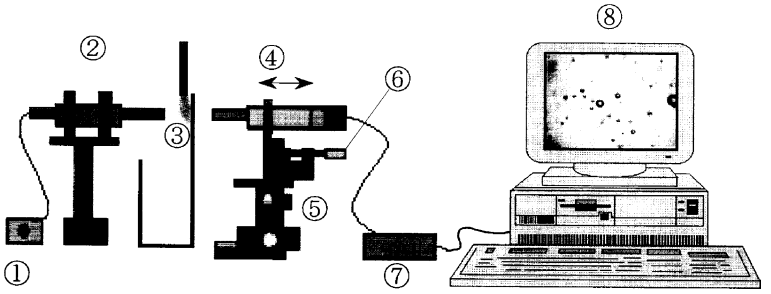

① Halogen light source
② Lamp
③ Bubbly water
④ CCD camera
⑤ Adjustable camera support
⑥ Micrometer head
⑦ Camera controller
⑧ Computer

Fig. 2. Measuring system of micro-air-bubbles.

2.2. Measurement of micro-air-bubbles

Fig. 2 shows the measuring system of micro-air-bubbles generated in the separation section. A CCD camera is used to take photographs of them. The camera has standing image pixels of 768(H)×493(V), and 525 vertical scanning lines and 470TV horizontal resolution lines. A halogen light source guided by an optical fiber is used and the camera exposure time is adjustable from 1/250 s to 1/10,000 s.

Micro-air-bubbles contained in water are observed continuously using the CCD camera with a main zoom lens of 4.5 times enlargement and an auxiliary one of three times at the exposure speed of 1/10,000 s. Moving pictures are transmitted to a personal computer via an image board and they are saved as animation files of 640×480 pixel/frame. Images sampled randomly from the files are saved as separated image files in the bitmap format. Then, the diameter and the number density of micro-air-bubbles are measured from these images after the removal of noise. Micro-air-bubbles within and outside a measuring domain are distinguished according to the image density of gray level, and the diameter is then correlated according to the relation obtained by calibration test. The test is done by the copper wire of 66.7 μm in diameter, which is put at different positions from the focus position of the CCD camera. The relative error of diameter measurement is estimated to be within 6% through uncertainty analysis of the above measuring system (Zhang et al., 2000).

As main parameters of micro-air-bubbles, the mean diameter and the number density of bubbles are adopted and these are measured in the measuring domain of 258 μm in height, 344 μm in width and 200 μm in depth, close to the exit of the separation section. Here, the distribution of micro-air-bubbles is thought to be uniform. The mean diameter d is defined as follows:

$$d = \frac{1}{n_b} \sum_{i=1}^{n_b} d_i, \tag{1}$$

where n_b denotes the number of micro-air-bubbles and d_i the diameters of a bubbles i in the measuring domain. The number density B is defined by,

$$B = \frac{n_b}{V_c}, \tag{2}$$

where V_c denotes the volume of the domain. Then, the bubble generation rate G is defined as follows:

$$G = Q_b B, \tag{3}$$

where Q_b denotes the flow rate of the bubbly water in the separation section.

3. Theoretical consideration of bubble detachment from porous plate

3.1. Forces acting on one bubble rotating together with porous plate

In this section, we discuss the relation between the rotational frequency of the porous plate and the size of bubbles formed on its surface on the basis of a simplified model. Generally, the detachment of bubbles from the porous plate is influenced by the water flow velocity in the dispersion box. In the present case, the velocity in the dispersion box is very small compared with the rotational one of the porous plate, and the influence of the water flow is negligible. We thus pay attention to one bubble rotating together with the plate, and the following assumptions are made. (1) The water around the porous plate is still. (2) The bubble connected to the plate is in an infinite water volume. (3) The bubble is spherical. (4) Air density within the bubble is negligibly small compared with the water density. (5) Airflow rate into the bubble is constant (Miyahara et al., 1982).

Fig. 3 shows forces acting on one spherical bubble rotating together with the porous plate, in which $\vec{F}_A$, $\vec{F}_B$, $\vec{F}_C$ and $\vec{F}_R$ denote the centrifugal force, the buoyancy force, the viscous drag (Batchelor, 1990) and their resultant force, respectively. The symbol r denotes the distance from the bubble center to the rotation axis. The magnitudes of $\vec{F}_A$, $\vec{F}_B$ and $\vec{F}_C$ can be given as,

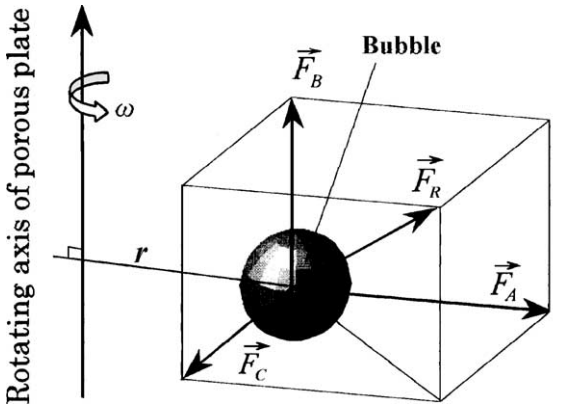

Fig. 3. Forces acting on bubble due to rotation of porous plate.

$$\begin{cases} F_A = 2\pi\rho R_b^3\omega^2 r/3, \\ F_B = \frac{4}{3}\pi\rho g R_b^3, \\ F_C = 12\pi\mu\omega r R_b, \end{cases} \tag{4}$$

where R_b denotes the bubble radius, ω the angular speed of the plate, g the gravity acceleration, ρ the water density and μ the water viscosity. The magnitude of the resultant force is therefore given by,

$$F_R = 2\pi R_b\sqrt{\frac{\rho^2 R_b^4}{9}(\omega^4 r^2 + 4g^2) + (6\mu\omega r)^2}. \tag{5}$$

The bubble grows with time by the supply of air through the hole on the plate, and its center moves in the direction of the force $\vec{F}_R$. Fig. 4 shows the schematic diagram of the bubble detaching from the hole on the porous plate: (a) a photograph of the detaching bubble taken by high speed video camera under condition of $n = 60$ rpm and $r = 25$ mm, (b) a schematic model of the bubble in detaching process. The figure shows a contracted throat at the connection between the bubble and the hole. Similar results have been also reported in several other papers (Onari, 1997; Akatsu and Nakamana, 1996; Chiba and Takahashi, 1998; Takahashi et al., 1980).

Because the detaching process of the bubble is unsteady, the bubble receives the resistance in the opposite direction of its movement owing to the added mass force $\vec{F}_r$ (Zuber, 1964; Sherwood, 1999; Michel and Belahadji, 1997). The magnitude of the force is,

$$F_r = \frac{2}{3}\pi\rho R_b^2(\dot{V}R_b + 3V\dot{R}_b), \tag{6}$$

in which V denotes the moving velocity of the bubble center that will be assumed equal to the growth speed of the bubble, $\dot{R}_b = dR_b/dt$ where t is the time. Then, we obtain $V = \dot{R}_b = q/4\pi R_b^2$ and $\dot{V} = dV/dt$, where q denotes the volumetric flow rate through a hole on the porous plate. The magnitude of $\vec{F}_r$ can be then written as,

$$F_r = \frac{\rho q^2}{24\pi R_b^2}. \tag{7}$$

The force attaching the bubble to the plate, on the other hand, can be given by,

$$F_\sigma = \pi d_0\sigma, \tag{8}$$

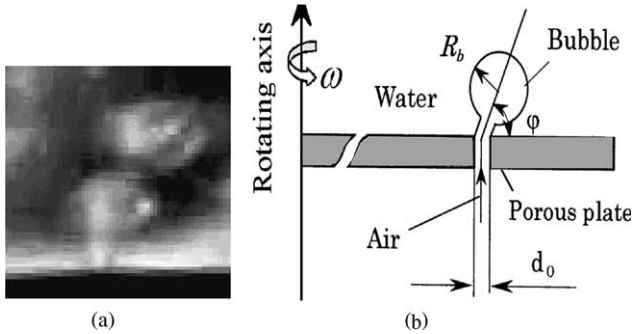

Fig. 4. Bubble detaching from rotating porous plate. (a) Photograph of bubbles and (b) model of bubble detachment.

where σ denotes the coefficient of surface tension and d_0 the diameter of the hole on the porous plate.

From the balance of all the forces, we obtain,

$$2\pi R_b \sqrt{\frac{\rho^2 R_b^4}{9}(\omega^4 r^2 + 4g^2) + (6\mu\omega r)^2} - \frac{\rho q^2}{24\pi R_b^2} = \pi d_0 \sigma. \tag{9}$$

The bubble radius is found to be dependent on the air flow rate q, the angular speed ω and the distance r.

3.2. Estimation of bubble diameter

Based on the above analysis, the size of the bubble detaching form the porous plate is discussed in relation to the rotational frequency $n(=\omega/2\pi)$ of the plate. Fig. 5 shows the radius of the

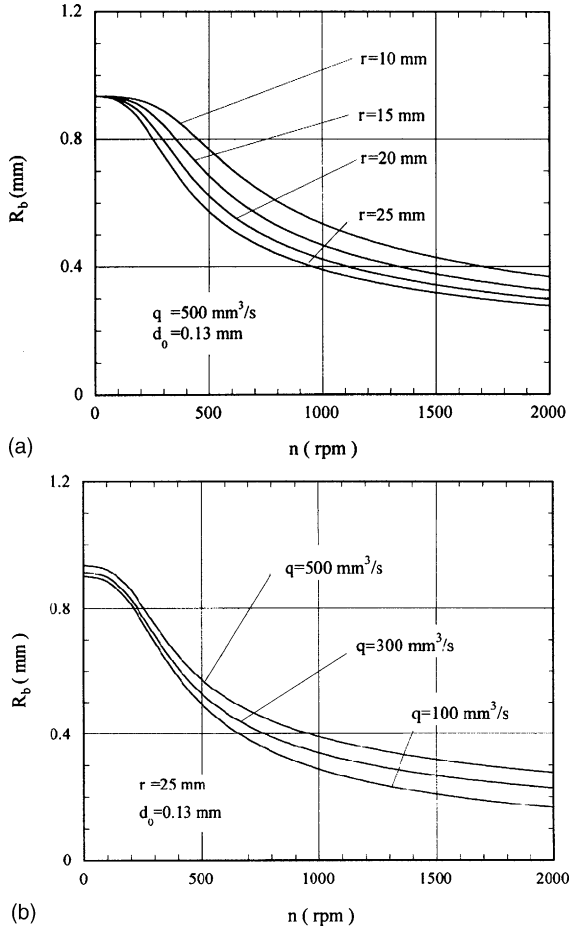

Fig. 5. Effect of rotational frequency on radius of bubble detaching from porous plate: (a) At different positions for $q = 500$ mm^3/s and $d_0 = 0.13$ mm and (b) at different air flow rates for $r = 25$ mm and $d_0 = 0.13$ mm.

bubble detaching from the plate, where (a) represents the bubble radius at different positions of bubble detachment when $q = 500$ mm^3/s and $d_0 = 0.13$ mm, and (b) does the bubble radius at different air flow rates when $r = 25$ mm and $d_0 = 0.13$ mm. For the both cases, the bubble radius decreases with the increase of the rotational frequency. At a more distant position from the rotation axis, the bubble radius becomes smaller because of the increase of the tangential speed. At the smaller air flow rate, the radius becomes smaller because of the smaller growth rate of the bubble.

4. Experimental results and discussion

4.1. Bubble generation in dispersion box

Fig. 6 shows the effect of the rotational frequency of porous plate on the radii of bubbles formed at the plate surface for $r = 25$ mm, $d_0 = 0.13$ mm and $q = 463$ mm^3/s. The solid line is the theoretical result calculated by Eq. (9) and the symbols ▲ and ● respectively denote experimental ones for $Q_w = 0$ and 87.5 cm^3/s where Q_w is the water flow rate. For $Q_w = 0$, the theoretical result and the experimental one are in rather good agreement. For $Q_w = 87.5$ cm^3/s, however, the experimental result deviates from the theoretical one because of the influence of the water flow rate. Estimating the growth time T of a bubble until its complete detachment from the plate surface, we get,

$$\frac{4}{3}\pi R_b^3 = qT. \tag{10}$$

When the air flow rate q is kept constant, the growth time becomes shorter with the increase of the rotational frequency. Thus, as shown in Fig. 5, the bubble radius decreases with the increase of the

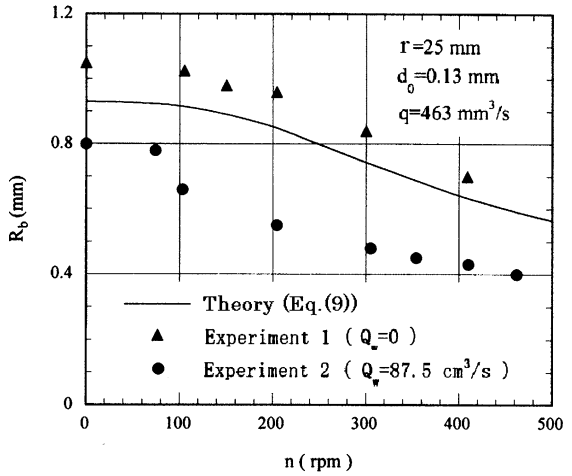

Fig. 6. Comparison between calculated and measured results of bubble radius ($d_0 = 0.13$ mm, $r = 25$ mm, $q = 463$ cm^3/s).

Fig. 7. Air-bubbles detaching from porous plate in dispersion box.

rotational frequency. Fig. 7 is a photograph of air-bubbles detaching from the plate surface. Bubbles of 0.4–0.8 mm in radius are generated under the same experimental condition as in Fig. 6.

4.2. Air dissolution in mixing box

Bubbles in the dispersion box are transported together with the surrounding water to the following mixing box in which air within the bubbles dissolves into water. Fig. 8 shows the flow state of bubbly water in the mixing box. The flow at the entrance located at the upper left corner of the mixing box is a jet flow in turbulent states. Bubbles are deformed in such a situation and break up. The total surface area of bubbles increases after the breakup. In the flow of water

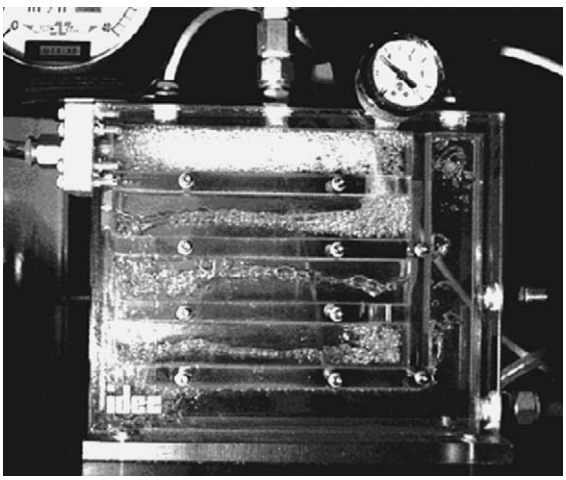

Fig. 8. Flow of water and air-bubbles in mixing box.

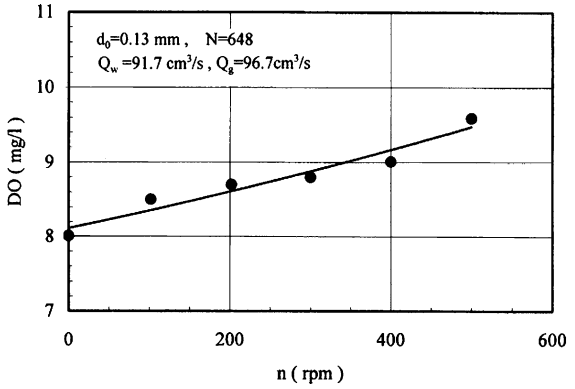

Fig. 9. Oxygen concentration in water varying with rotational frequency ($d_0 = 0.13$ mm, $N = 648$, $Q_w = 91.7$ cm^3/s, $Q_g = 96.7$ cm^3/s).

containing numerous air-bubbles, the rate of air dissolution into the surrounding water is proportional to the total surface area of bubbles, and it increases with the decrease of the bubble diameter because not only the total surface area but also the mass transport coefficient increase (Mori et al., 1977; Takemura and Yabe, 1997). In fact, Hammerton and Garner (1954) have found that the smaller becomes the bubble diameter, the faster does the air dissolution rate.

Fig. 9 shows the degree of air dissolution in water versus the rotational frequency of the porous plate. The abscissa denotes the rotational frequency n (rpm) and the ordinate the dissolved-oxygen concentration DO (mg/l). The experimental condition is as follows: water temperature (T_w) = 28.5 °C, pressure in mixing box (P_B) = 0.45 MP$_a$, pressure in the separation section just after pressure reduction valve (Ps) = 0.1 MP$_a$, dissolved-oxygen concentration of water in supply water tank (DO_t) 4.7 mg/l, water flow rate (Q_w) = 91.7 cm^3/s, air flow rate (Q_g) = 96.7 cm^3/s, $d_0 = 0.13$ mm, and $N = 648$.

The dissolved-oxygen concentration is measured at the exit of the pressure reduction valve. The concentration increases in proportion to the rotational frequency. By the use of the rotating porous plate, the oxygen is dissolved by 1.7–2.0 times in concentration compared with the one in water supply tank. The reason is thought to be as follows. As the rotational frequency increases, bubbles detaching from the porous plate surface become smaller, and the bubble number increases. This means that the total surface area of bubbles becomes larger, therefore, the amount of oxygen dissolved into the surrounding water increases. This also suggests that the concentration of air in the water increases.

4.3. Effect of rotational frequency on characteristics of micro-air-bubbles

In order to evaluate the performance of the present micro-air-bubble generator, we measured the mean diameter and the number density of micro-air-bubbles at the distance of 160 mm downstream from the reduction valve by changing the rotational frequency of the porous plate and the air flow rate ejected to water. Fig. 10 shows the effect of rotational frequency on the mean diameter and the number density of micro-air-bubbles under the condition of $d_0 = 0.14$ mm, $N = 126$, $Q_w = 66.7$ cm^3/s, $Q_g = 76.5$ cm^3/s and $P_B = 0.35$ MPa. The figure demonstrates that the

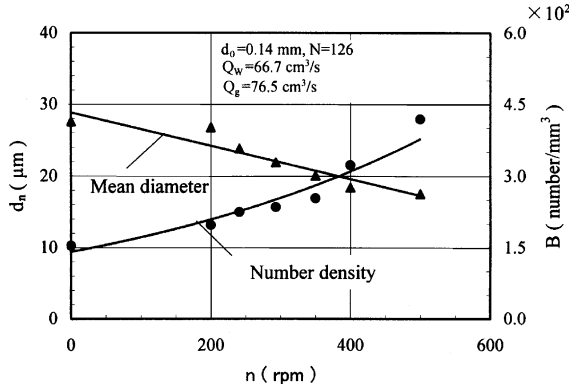

Fig. 10. Effect of rotational frequency on mean diameter and number density ($d_0 = 0.14$ mm, $N = 126$, $Q_w = 66.7$ cm^3/s, $Q_g = 76.5$ cm^3/s).

mean diameter decreases and the number density increases with the increase of the rotational frequency as expected. The reason is that not only the diameter of bubbles detached from the porous plate decreases but also the number of bubbles increases. Therefore, the total surface area of bubbles and the mass transportation coefficient through bubble surfaces increase, and the amount of air dissolution to water consequently increases. This result shows that it is possible to control the mean diameter and the number density of bubbles to a certain extent by adjusting the rotational frequency.

The number of bubbles generated in a unit time called as the generation rate is an important index of micro-air-bubble generation performance of the apparatus. Its variation with the rotational frequency of the porous plate is investigated. Fig. 11 shows the relation between the

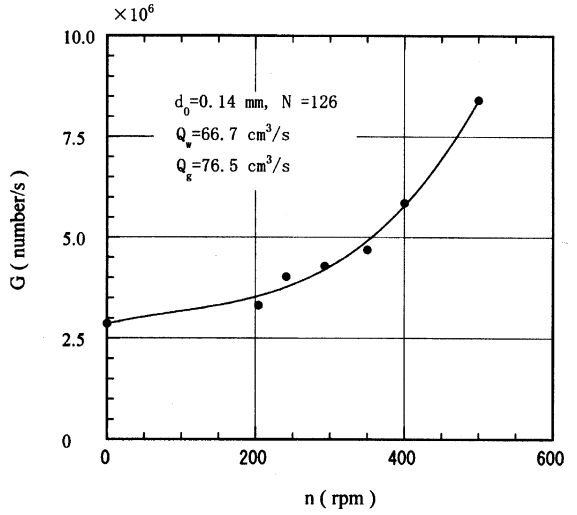

Fig. 11. Effect of rotational frequency on bubble generation rate ($d_0 = 0.14$ mm, $N = 126$, $Q_w = 66.7$ cm^3/s, $Q_g = 76.5$ cm^3/s).

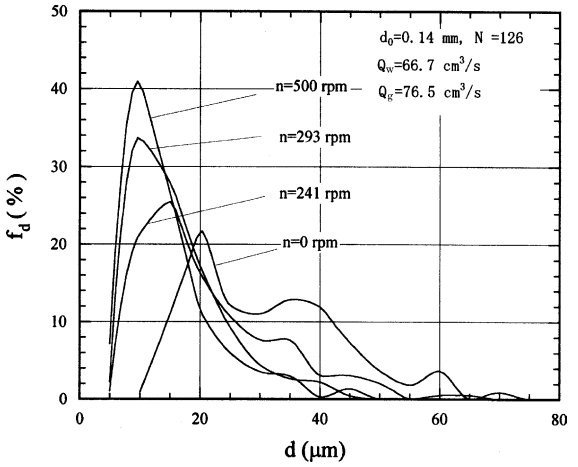

Fig. 12. Distribution of bubble diameter under different rotational frequencies ($d_0 = 0.14$ mm, $N = 126$, $Q_w = 66.7$ cm^3/s, $Q_g = 76.5$ cm^3/s).

micro-air-bubble generation rate and the rotational frequency under the same condition as the above. The variation tendency is similar to the number density. Fig. 12 shows the distribution of bubble diameter for different rotational frequencies of $n = 0$, 241, 293 and 500 rpm at the same experimental condition as the above. The abscissa denotes the bubble diameter and the ordinate does the statistic counting of bubbles in percentage. The result demonstrates that the percentage of large bubbles decreases with the increase of the rotational frequency, the mean diameter of micro-air-bubbles decreases, and the distribution of air-bubble diameters trends to be much more uniform.

4.4. Effect of air flow rate on characteristics of micro-air-bubbles

Fig. 13 shows the effect of air flow rate on the mean diameter of micro-air-bubbles for different rotational frequencies. The porous plate with $d_0 = 0.14$ mm and $N = 648$ is used because it is expected to increase the number density of bubbles formed in the bubble dispersion box. Under a given air flow rate, the mean diameter decreases with the increase of the rotational frequency. Under a given rotational frequency, the mean diameter increases with the increase of the air flow rate. For a low rotational frequency, the mean diameter increases sharply. But for a higher rotational frequency, it increases slowly. Thus, it is important to increase the rotational frequency in order to enhance the number density by increasing the air flow rate and suppress the mean diameter of micro-air-bubbles.

Fig. 14 shows the effect of air flow rate on the number density for different rotational frequencies. For a given rotational frequency, the number density increases with the air flow rate. For a given air flow rate, the number density increases with the rotational frequency. The reason may be due to that the number of bubbles detaching from the plate surface increases with the increase of air flow rate so that the total surface area of the bubbles increases. Therefore, the air

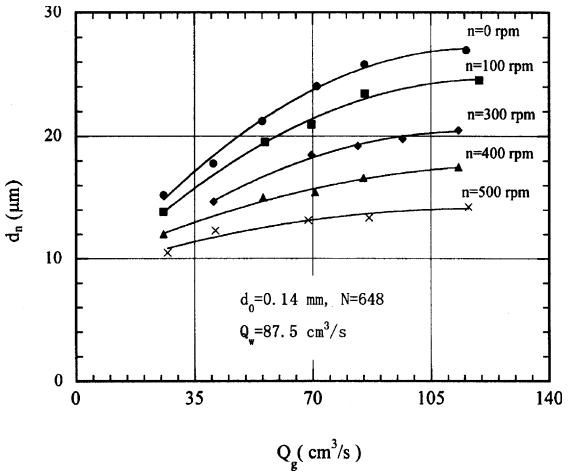

Fig. 13. Relations between mean diameter of bubbles and air flow rate for different rotational frequencies ($d_0 = 0.14$ mm, $N = 648$, $Q_w = 87.5$ cm^3/s).

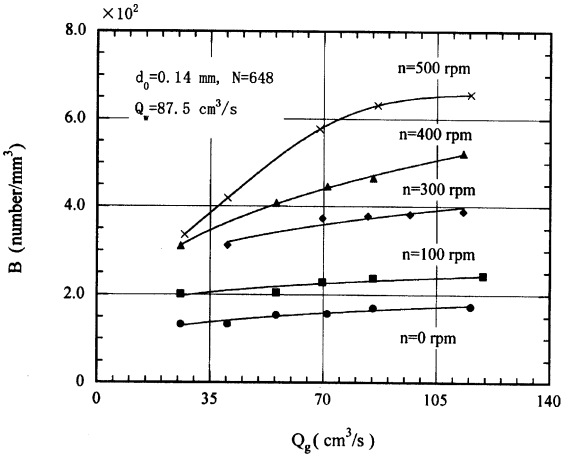

Fig. 14. Relations between bubble number density and air flow rate for different rotational frequencies ($d_0 = 0.14$ mm, $N = 648$, $Q_w = 87.5$ cm^3/s).

dissolution into water is enhanced and the number density of the bubbles increases. To confirm this conjecture, we measured the oxygen concentration of water in the separation section by changing the air flow rate ejected to water. Fig. 15 shows the relation between the oxygen concentration and the air flow rate under the condition of $d_0 = 0.13$ mm, $N = 648$, $Q_w = 91.7$ cm^3/s, $n = 500$ rpm and $DO_t = 4.7$ mg/l. The oxygen concentration surely increases with the increase of air flow rate.

When the air flow rate and the rotational frequency are increased at the same time, the mass transport coefficient increases further because the diameter of bubbles is smaller compared with

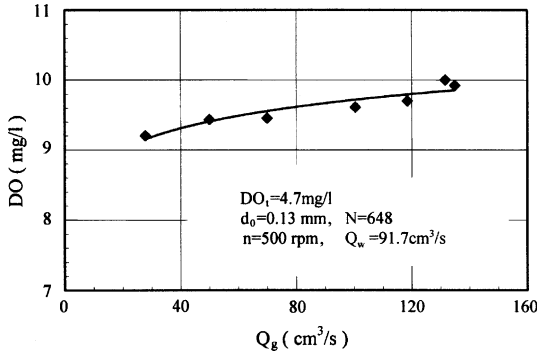

Fig. 15. Oxygen concentration in bubbly water varying with air flow rate ($d_0 = 0.13$ mm, $N = 648$, $Q_w = 91.7$ cm^3/s, $n = 500$ rpm, $DO_t = 4.7$ mg/l).

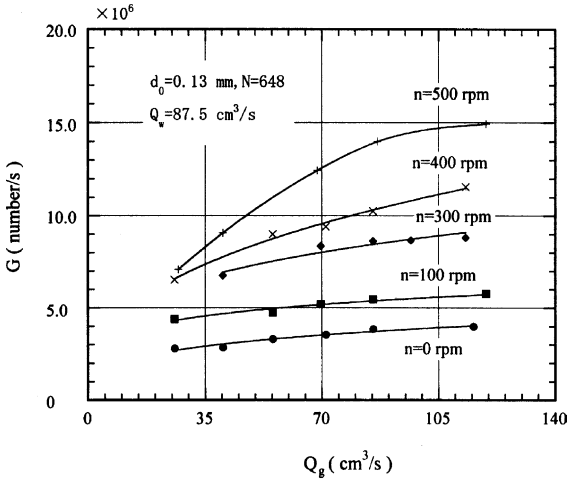

Fig. 16. Effect of air flow rate on bubble generation rate ($d_0 = 0.13$ mm, $N = 648$, $Q_w = 87.5$ cm^3/s).

the case of the increase of the air flow rate alone and the number of bubbles ejected to water becomes greater compared with the rotational frequency alone. So, the air dissolution increases remarkably and the number density of micro-air-bubbles becomes much higher. Fig. 16 shows the variation of bubble generation rate with the air flow rate for given rotational frequencies. As the opening of pressure reduction valve is kept constant, the flow rate of bubbly water out of the exit is nearly constant (Hinze, 1955). Thus the variation of micro-air-bubble generation rate is approximately similar to the variation of the number density shown in Fig. 14. Compared with the bubble generation rate ($G \leqslant 3.57 \times 10^6$ number/s) of the other methods (Machitani et al., 1995), the generation rate of the present new device is prominently proved to be much higher.

5. Conclusions

In order to reduce the mean diameter and to increase the number density of micro-air-bubbles, the new device of micro-air-bubble generation has been developed. The results are summarized as follows.

(1) The size of bubbles detaching from the porous plate has a large influence on the air dissolution in water. As the diameter of air-bubbles ejected into water decreases, the air dissolution rate increases and the final size of micro-air-bubbles in bubbly water decreases.
(2) With the increase of the rotational frequency of the porous plate and the flow rate of are ejected into water, the diameter of micro-air-bubbles decreases remarkably.
(3) The number density of micro-air-bubbles is enhanced by increasing the air flow rate, but the diameter of the bubbles also increases. The increase of bubble diameter can be suppressed by increasing the rotational frequency of the porous plate.

References

Akatsu, Y., Nakamana, S., 1996. Visualization of behavior of single-bubble growth and bubble coalescence. J. Visualization Soc. Jpn. 16, 258–265 (in Japanese).

Batchelor, G.K., 1990. Fluid Dynamics. Cambridge University Press, London. pp. 402–409.

Cheremisinoff, N.P. (Ed.), 1985. Encyclopedia of Fluid Mechanics. In: Gas–Liquid Flows, vol. 3. World Scientific Publishing, London, pp. 351–359.

Chiba, N., Takahashi, Y., 1998. Generation of Micro Air Bubbles of Uniform Size in Water, Proceedings of the Third International Symposium on Cavitation, Grenoble, pp. 91–94.

Hammerton, D., Garner, F.H., 1954. Gas absorption from single bubble. Trans. Instn. Chem. Engrs. 32, S18–S21.

Hinze, J.O., 1955. Fundamentals of the hydrodynamic mechanism of splitting in dispersion processes. AIChE J. 1, 289–295.

Iguchi, M., Chihara, T., 1997. Experimental investigation of bubble formation from a nozzle and orifice (1st report). Japanese J. Multiphase Flow 11, 46–55 (in Japanese).

Machitani, K. et al., 1995. Study of bubbly water (in Japanese). IDEC Rev., 1–9.

Michel, J.M., Belahadji, B., 1997. In: Fundamentals of Cavitation. Brasilia University Press, pp. 46–47.

Miyahara, T., Aizawa, K., Tajahashi, T., 1991. Oxygen dissolution into water under elevated air pressure condition. Water Purif. Liquid Wastes Treat. 32, 9–15 (in Japanese).

Miyahara, T., Matsuba, Y., Takahasi, T., 1982. Size of bubbles generated from perforated plates. Collected Papers Chem. Eng. 8, 13–17 (in Japanese).

Mori, Y. et al., 1977. Fundamental study of bubble dissolution in liquid. Int. J. Heat Mass Transfer 20, 41–50.

Onari, H., 1997. Waste water purification in wide water area by use of micro-bubble techniques. Japanese J. Multiphase Flow 11, 263–266 (in Japanese).

Sherwood, J.D., 1999. The force on a growing bubble in potential flow. Int. J. Multiphase Flow 25, 705–709.

Takahashi, T. et al., 1979. Fundamental study of bubble formation in dissolved air pressure flotation. J. Chem. Eng. Jpn. 12, 275–280.

Takahashi, T. et al., 1980. Bubble formation at submerged nozzles in concurrent. Countercurrent and crosscurrent flow. Collected Papers Chem. Eng. 6, 563–569 (in Japanese).

Takemura, F., Yabe, A., 1997. Rising speed and dissolution rate of carbon dioxide bubble in slightly contaminated water. J. Fluid Mech. 378, 319–334.

Zhang, R. et al., 2000. A study of the measurement of micro bubbles in micro bubble formation device. Japanese J. Multiphase Flows 14, 329–338 (in Japanese).
Zuber, N., 1964. On the dispersed two-phase flow in the laminar-flow regime. Chem. Eng. Sci. 19, 897–917.